

dy. 39

FED LIBRARY ACQUISITION 1979

OAK RIDGE NATIONAL LABORATORY LIBRARIES



3 4456 0536804 5

Electron Impact Ionization of Multicharged Ions

D. H. Crandall
R. A. Pheneuf
D. C. Gregory

FUSION ENERGY DIVISION LIBRARY

OAK RIDGE NATIONAL LABORATORY
OPERATED BY UNION CARBIDE CORPORATION - FOR THE DEPARTMENT OF ENERGY

Printed in the United States of America. Available from
National Technical Information Service
U.S. Department of Commerce
5285 Port Royal Road, Springfield, Virginia 22161
NTIS price codes—Printed Copy A03; Microfilm A01

This report was prepared as a result of work sponsored by an agency of the United States Government. Neither the United States nor any agency thereof, nor any of their employees, makes any warranty, expressed or implied, or assumes any legal liability or responsibility for any third party's use or the results of such use of any information appearing in this report, or for any damages (including those resulting from the use of any information appearing in this report) that may be caused by the use of the information contained herein.

Contract No. W-7405-eng-26

Electron Impact Ionization of Multicharged Ions

D. H. Crandall, R. A. Phaneuf, and D. C. Gregory

Date Published: September 1979

Physics Division

Oak Ridge National Laboratory
Oak Ridge, Tennessee 37830
operated by
Union Carbide Corporation
for the
Department of Energy

Abstract

This report presents original experimental data in tabular and graphical form for electron impact ionization cross sections of the ions B^{3+} , C^{3+} , C^{4+} , N^{3+} , N^{4+} , N^{5+} , O^{3+} , O^{4+} , O^{5+} , and Ar^{4+} for energies between the ionization thresholds and 1500 eV, with absolute accuracy varying between $\pm 6\%$ and $\pm 17\%$. At present there are no other measurements of comparable accuracy for ions of initial charge greater than $2+$. Calculated cross sections from the Lotz formula and scaled-Coulomb-Born prescription are compared with the data. Ionization rate coefficients for plasmas with Maxwellian electron energy distribution were computed from the measured cross sections for each ion species. These rates are compared with available theoretical and measured plasma ionization rates.

Acknowledgments

This research was funded through the Division of Chemical Sciences of the Department of Energy's Office of Basic Energy Sciences. In addition, funding for some of the personnel (R. A. Phaneuf) and equipment was provided through the Office of Fusion Energy of DOE. D. C. Gregory (present address - 901A Tandem Building, Brookhaven National Laboratory, Upton, NY 11973) performed some of his work on this project while appointed as a research associate at the Joint Institute for Laboratory Astrophysics (JILA) at the University of Colorado, Boulder, Colorado. The continuing collaboration of G. H. Dunn and others of JILA on the closely related project of electron impact excitation of multicharged ions has provided expertise and some specialized equipment used directly in the present project. P. O. Taylor (presently at Center for Astrophysics, 60 Garden Street, Cambridge, MA 02138) contributed significantly to the development of the apparatus and the first measurements while appointed as a research associate at JILA. B. E. Hasselquist and F. W. Meyer helped with computer programming, and J. W. Hale provided technical assistance in maintenance and operation of equipment. The continuing interest and guidance of C. F. Barnett (Group Leader) and P. H. Stelson (Division Director) and the editorial assistance of S. W. Hawthorne are also gratefully acknowledged.

Table of Contents

ABSTRACT	iii
ACKNOWLEDGMENTS	v
1. INTRODUCTION	1
2. RESULTS	4
2.1 Cross Sections	4
2.2 Ionization Rates	19
3. CONCLUSION	26
REFERENCES	27

Electron Impact Ionization of Multicharged Ions

1. Introduction

Electron impact ionization (together with electron-ion recombination) controls the state of ionization of ions occurring in high temperature plasmas and thus indirectly determines many of the plasma properties (conductivity and light radiated, for examples). There are several theoretical approximations used to estimate ionization cross sections, but there have been little data of sufficient accuracy to test the reliability of these estimates for ions of initial charge greater than $2+$. The experimental data presented here were acquired both to test available theory and for direct use in plasma physics.

The experiments were carried out with crossed beams of electrons and ions as shown schematically in Fig. 1. The ion source¹ is the prototype of the source used in the Oak Ridge Isochronous Cyclotron (ORIC), and the electron gun is modeled after that developed by Taylor et al.² for use in crossed-beams experiments at the Joint Institute for Laboratory Astrophysics (JILA), Boulder, Colorado. Details of the experimental geometry are given in references 3 and 4, which present the first ionization results obtained from this research project.

Theories of electron impact ionization date to the 1912 work of J. J. Thomson,⁵ and, in fact, the most commonly used theoretical estimate is a semiempirical adjustment of the Thomson formula given by Lotz.⁶ Another modification of classical theory is the exchange classical impact parameter (ECIP) description,⁷⁻⁹ which, by specifically allowing for the known quantum phenomenon of exchange of the incident electron and a bound electron, reduces the ionization cross sections from those given by the purely classical formula of Thomson. Exact quantum mechanical

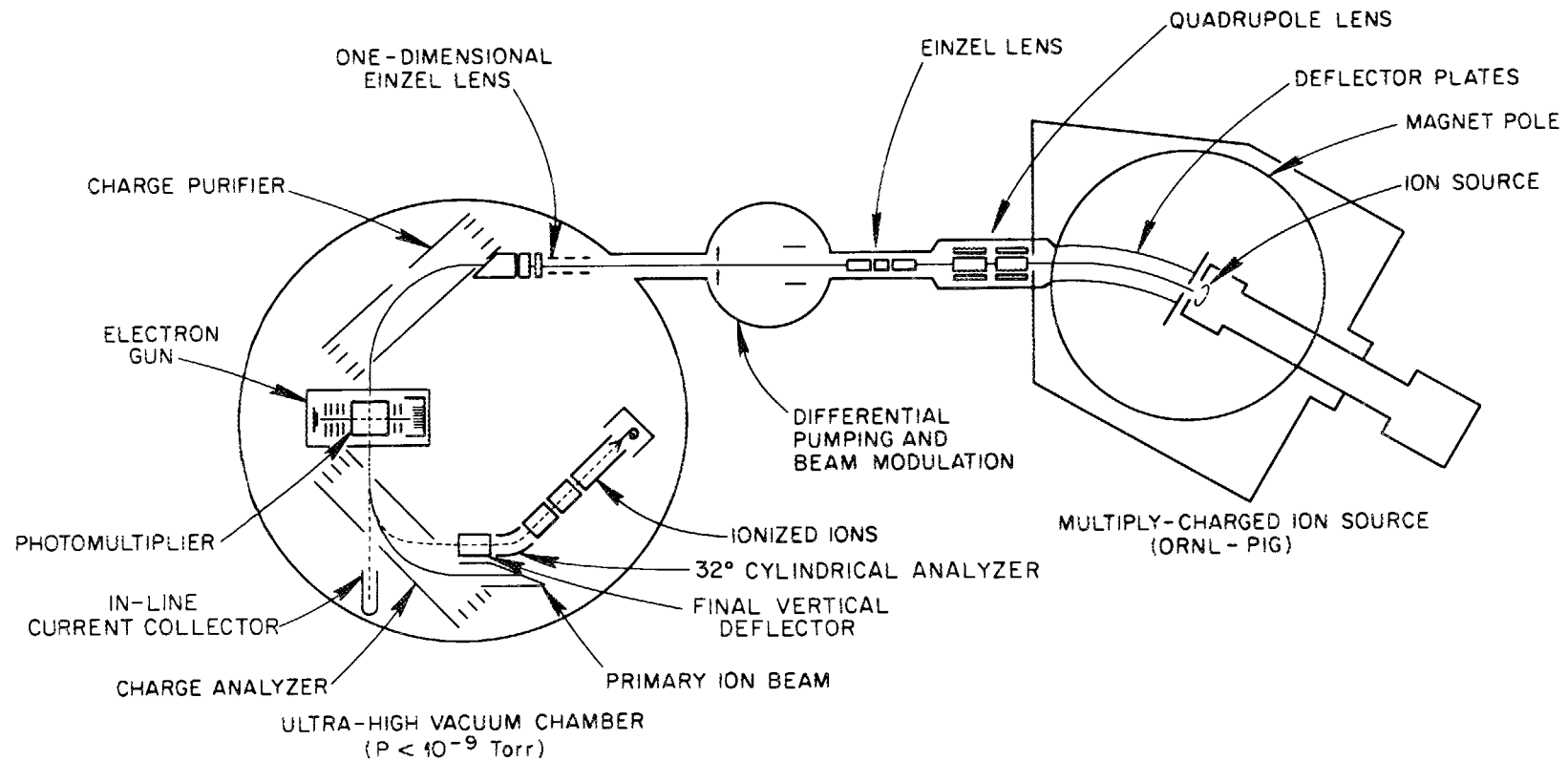


Fig. 1. Schematic of the apparatus.

representation of the ionization process has not been formulated. However, Born and Coulomb-Born quantum approximations have been developed and specifically calculated for a few of the ions studied in the present experiments.^{10,11} Recently, a prescription has been given for scaling the Coulomb-Born results for hydrogenic ions of infinite nuclear charge to cases of partially ionized multicharged ions. This scaled Coulomb-Born prescription¹² can be applied to all of the measured cases presented here (except Ar^{4+}).

In this report the measured cross sections for electron impact ionization of B^{3+} , C^{3+} , C^{4+} , N^{3+} , N^{4+} , N^{5+} , O^{3+} , O^{4+} , O^{5+} , and Ar^{4+} are compared with the commonly used Lotz formula, with the scaled Coulomb-Born formula, and, for the few published cases available, with the specific Coulomb-Born calculations. Ionization rate coefficients, calculated from the present cross section data integrated with a Maxwellian distribution of plasma electrons, are compared with rates given by the Lotz and scaled-Coulomb-Born formulas. Few details of experimental technique or underlying physics and comparison with other work are presented here, but have been^{3,4} and will be discussed in open literature publications on this research. The results presented here should be immediately useful for plasma physics research and for comparison with developing theories of electron impact ionization and excitation of multicharged ions.

2. Results

2.1. Cross Sections

The Lotz formula has been specifically taken to be:

$$\sigma(E) = 4.5 \times 10^{-14} \sum_j \frac{r_j}{I_j E} \ln\left\{\frac{E}{I_j}\right\} \text{ cm}^2,$$

where r_j is the number of electrons in level j , I_j is ionization energy of that level in eV, and E is the collision energy in eV. The ionization energies I_j for inner shells can be obtained from the calculations of Clementi and Roetti.¹³ The scaled Coulomb-Born results are calculated according to the Golden and Sampson prescription.¹² In Figs. 2-11 the measured cross sections are compared with values calculated from these two prescriptions. Tables 1-3 present the measured cross section values.

For Li-like ions the incident beams contain purely ground state ions. For He-like ions there may be as many as 1% of B^{3+} ions in the metastable $1S$ and $3S$ states, but for C^{4+} and N^{5+} the beams should contain no more than 0.1% metastables. However, O^{3+} , N^{3+} , and O^{4+} beams contain significant fractions of incident ions in metastable states. For O^{3+} the fraction of metastables is estimated to be 16% in the $(1s^2 2s 2p^2) 4P$ state. The estimate is obtained from the magnitude of the observed cross section between the 68.6-eV threshold for ionization of the metastable ions and the 77.4-eV threshold for ionization of the ground state ions. Since the cross section for ionization out of the ground and metastable states is expected to be nearly the same for this case, no correction of the data or theories has been applied. For N^{3+} and O^{4+} (Be-like ions) the fraction of ions in the $(1s^2 2s 2p) 3P$ metastable state is roughly 50%, and the theoretical cross sections for ionization

out of this state are significantly larger than for ionization out of the $(1s^2 2s^2) \ ^1S$ ground state. Thus the theories have been calculated for a 50-50 mixture of these states for comparison with the present N^{3+} and O^{4+} data.

The inner-shell excitation-autoionization contribution to the total ionization cross sections is apparent in the C^{3+} , N^{4+} , O^{5+} , O^{4+} , and Ar^{4+} cases. The onset of excitation-autoionization causes an abrupt increase in the ionization cross sections at energies above the peaks in the direct ionization. For the C^{3+} case (Fig. 2) the sum of excitation cross sections $1s^2 2s \rightarrow 1s 2s 2\ell$ has been calculated by J. B. Mann¹⁴ and added to the scaled Coulomb-Born ionization calculation beginning at the 294-eV excitation threshold. Comparison of this theoretical excitation result and present data assumes that all of the inner-shell excitation decays by autoionization before the ions are charge analyzed in the experiment (within about 0.3 μ sec). The excitation cross sections $1s^2 2s \rightarrow 1s 2s 2\ell$ have recently been calculated by R. J. W. Henry²¹ for C^{3+} , N^{4+} , and O^{5+} , and good agreement is obtained with the increase in ionization cross section observed in the present data for C^{3+} and N^{4+} , but for O^{5+} the predicted excitation contribution is significantly smaller than in present data. This process may be more significant for higher charge states and particular electronic configurations.^{4,18-22} The process was specifically anticipated near 550 eV in the O^{3+} case (Fig. 9) and near 420 eV in the N^{3+} case (Fig. 8) but was not discernible within statistical uncertainty of the data. The classical theory as calculated by Salop¹⁶ for Ar^{4+} (Fig. 11) includes excitation-autoionization and predicts structure in the ionization cross section similar to that found in the present experimental data near 250 eV.

Table 1. Ionization cross sections for Li-like ions for energies in threshold units (Figs. 2-4)

E/E_{th}	C^{3+} σ_{34} (10^{-18} cm 2) $E_{th} = 64.45$ eV	N^{4+} σ_{45} (10^{-18} cm 2) $E_{th} = 97.86$ eV	O^{5+} σ_{56} (10^{-18} cm 2) $E_{th} = 138.1$ eV
1.09	0.46 \pm .20 ^a	0.28 \pm .04	
1.17	1.07 \pm .20	0.56 \pm .08	0.31 \pm .18
1.25	1.20 \pm .19	0.74 \pm .04	
1.40	1.43 \pm .17	0.93 \pm .04	0.45 \pm .17
1.70		1.21 \pm .05	
2.00		1.27 \pm .05	
2.2	2.51 \pm .11		0.82 \pm .15
2.5		1.45 \pm .04	
3.0		1.47 \pm .04	0.75 \pm .10
3.6	2.59 \pm .04	1.40 \pm .04	0.67 \pm .05
4.0	2.37 \pm .05	1.47 \pm .05	0.76 \pm .05
4.2	2.40 \pm .04	1.33 \pm .04	0.84 \pm .10
4.4	2.33 \pm .04	1.41 \pm .04	
4.6	2.37 \pm .03	1.42 \pm .04	0.89 \pm .08
4.8	2.47 \pm .03	1.44 \pm .04	
5.0	2.49 \pm .04	1.46 \pm .04	0.88 \pm .12
5.25	2.39 \pm .04	1.42 \pm .04	
5.6		1.41 \pm .04	0.88 \pm .14
6.0	2.41 \pm .07	1.40 \pm .04	
7.0	2.25 \pm .06	1.35 \pm .04	0.74 \pm .36
8.0	2.10 \pm .11	1.30 \pm .02	0.70 \pm .14
10.0	2.00 \pm .07	1.22 \pm .03	0.48 \pm .10
12.0	1.92 \pm .08	1.16 \pm .04	
15.0	1.78 \pm .04	1.05 \pm .05	
18.3	1.47 \pm .08		
22.9	1.37 \pm .06		

^aThe uncertainties listed are 90% confidence level counting statistics. Additional systematic uncertainty of $\pm 6\%$ for C^{3+} and N^{4+} and of $\pm 10\%$ for O^{5+} should be added in quadrature with individual statistical uncertainty to obtain good confidence absolute uncertainty.

Table 2. Ionization cross sections for He-like ions for energies in threshold units (Figs. 5-7)

E/E_{th}	$\sigma_{34}^{B^{3+}}$ (10^{-19} cm ²) $E_{th} = 259.4$ eV	$\sigma_{45}^{C^{4+}}$ (10^{-19} cm ²) $E_{th} = 392.1$ eV	$\sigma_{56}^{N^{5+}}$ (10^{-19} cm ²) $E_{th} = 552.1$ eV
1.057	0.41 ± 0.16^a		
1.115	0.57 ± 0.16	0.30 ± 0.19	
1.25		0.39 ± 0.16	
1.30	1.51 ± 0.17		
1.43			0.85 ± 0.16
1.50	2.62 ± 0.18	1.17 ± 0.18	
1.75	3.15 ± 0.24	1.63 ± 0.26	1.21 ± 0.20
1.87	3.51 ± 0.11		
1.99	3.72 ± 0.23	1.77 ± 0.08	
2.15			1.37 ± 0.19
2.25	4.67 ± 0.19		
2.50		2.33 ± 0.20	
2.65	4.62 ± 0.19		1.06 ± 0.18
3.01	4.53 ± 0.12	2.20 ± 0.11	
3.59	4.85 ± 0.11		
3.77		2.34 ± 0.10	
4.16	4.74 ± 0.12		
4.92	4.14 ± 0.10		
5.69	3.99 ± 0.12		

^aListed uncertainties are one standard deviation counting statistics (67% confidence level). Additional systematic uncertainty of $\pm 10\%$ should be added in quadrature to obtain absolute uncertainty.

Table 3. Ionization cross sections for N^{3+} , O^{3+} , O^{4+} , and Ar^{4+} ions for energies in units of the ground state threshold energy (Figs. 8-11)

E/E_{th}	N^{3+} σ_{34} (10^{-18} cm 2) $E_{th} = 77.5$ eV ($E_{met} = 69.1$ eV)	O^{3+} σ_{34} (10^{-18} cm 2) $E_{th} = 77.4$ eV ($E_{met} = 68.6$ eV)	O^{4+} σ_{45} (10^{-18} cm 2) $E_{th} = 113.9$ eV ($E_{met} = 103.7$)	Ar^{4+} σ_{45} (10^{-18} cm 2) $E_{th} = 75.0$ eV ($E_{met} = 73.0$)
0.885	0.24 \pm .06 ^a	0.11 \pm .11	.09 \pm .09	
0.905	0.49 \pm .06	0.20 \pm .10		
0.94	0.75 \pm .04	0.36 \pm .13		
0.96	0.98 \pm .05	0.36 \pm .09	.37 \pm .09	.04 \pm .36
0.98	1.08 \pm .05	0.48 \pm .10	.47 \pm .09	
1.01	1.37 \pm .06	0.99 \pm .08		1.09 \pm .36
1.03	1.60 \pm .06	1.25 \pm .10	.79 \pm .09	
1.07	1.91 \pm .08	2.10 \pm .16		3.21 \pm .35
1.15	2.98 \pm .08	2.58 \pm .16	1.09 \pm .11	4.20 \pm .31
1.25		3.40 \pm .17	1.61 \pm .09	6.08 \pm .35
1.50	3.92 \pm .07	5.31 \pm .20	2.20 \pm .12	8.20 \pm .28
1.83	4.52 \pm .04	6.26 \pm .18	2.65 \pm .12	8.92 \pm .30
2.14		6.44 \pm .15	2.82 \pm .06	9.17 \pm .20
2.50	4.99 \pm .03	6.60 \pm .07	2.92 \pm .05	9.30 \pm .13
2.97		6.80 \pm .10	2.88 \pm .05	9.45 \pm .12
3.72	5.28 \pm .07	6.93 \pm .10	2.80 \pm .04	10.28 \pm .13
4.35		6.83 \pm .15	2.67 \pm .05	10.20 \pm .21
5.00	4.83 \pm .06	6.60 \pm .11	2.67 \pm .05	9.50 \pm .15
6.09	4.47 \pm .03		2.59 \pm .07	
6.25	4.45 \pm .03	6.17 \pm .18	2.50 \pm .07	8.35 \pm .18
7.50	4.22 \pm .06	5.60 \pm .13	2.21 \pm .04	7.96 \pm .18
8.70	4.10 \pm .06	5.17 \pm .14	2.04 \pm .04	7.48 \pm .18
10.10	3.70 \pm .05	4.91 \pm .14	1.87 \pm .04	6.88 \pm .17
11.37	3.57 \pm .05	4.62 \pm .09		6.42 \pm .18
13.00	3.15 \pm .05	4.19 \pm .08	1.46 \pm .04	5.88 \pm .18
15.20	2.86 \pm .05			5.35 \pm .18
16.50		3.57 \pm .11		5.04 \pm .18
19.06	2.32 \pm .05	3.14 \pm .10		4.44 \pm .18

^aThe listed uncertainties are 90% confidence level counting statistics for the individual data points. Additional systematic uncertainty of $\pm 6\%$ should be added in quadrature to obtain good confidence absolute uncertainty.

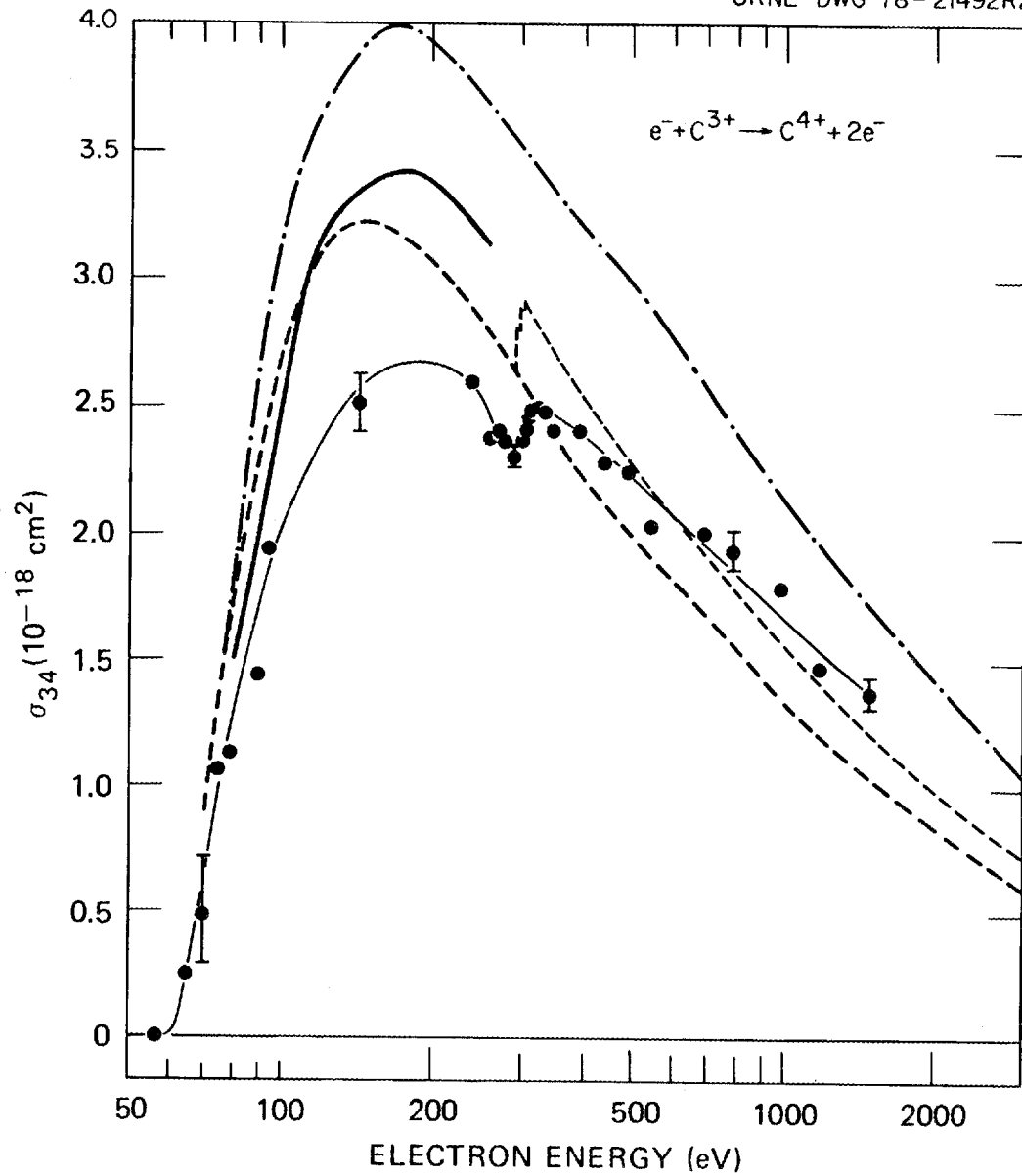


Fig. 2. Cross section for electron impact ionization of C^{3+} . Connected solid points are present data with 90% confidence level relative error bars (see Table 1 for absolute uncertainties). Solid curve is Coulomb-Born theory (Ref. 10); dashed curve is scaled Coulomb-Born theory (Ref. 12); dashed curve added beginning at 294 eV is $1s^2 2s \rightarrow 1s^2 2s n\ell$ excitation calculated by J. B. Mann (Ref. 14); dot-dashed curve is Lotz semiempirical formula (Ref. 6).

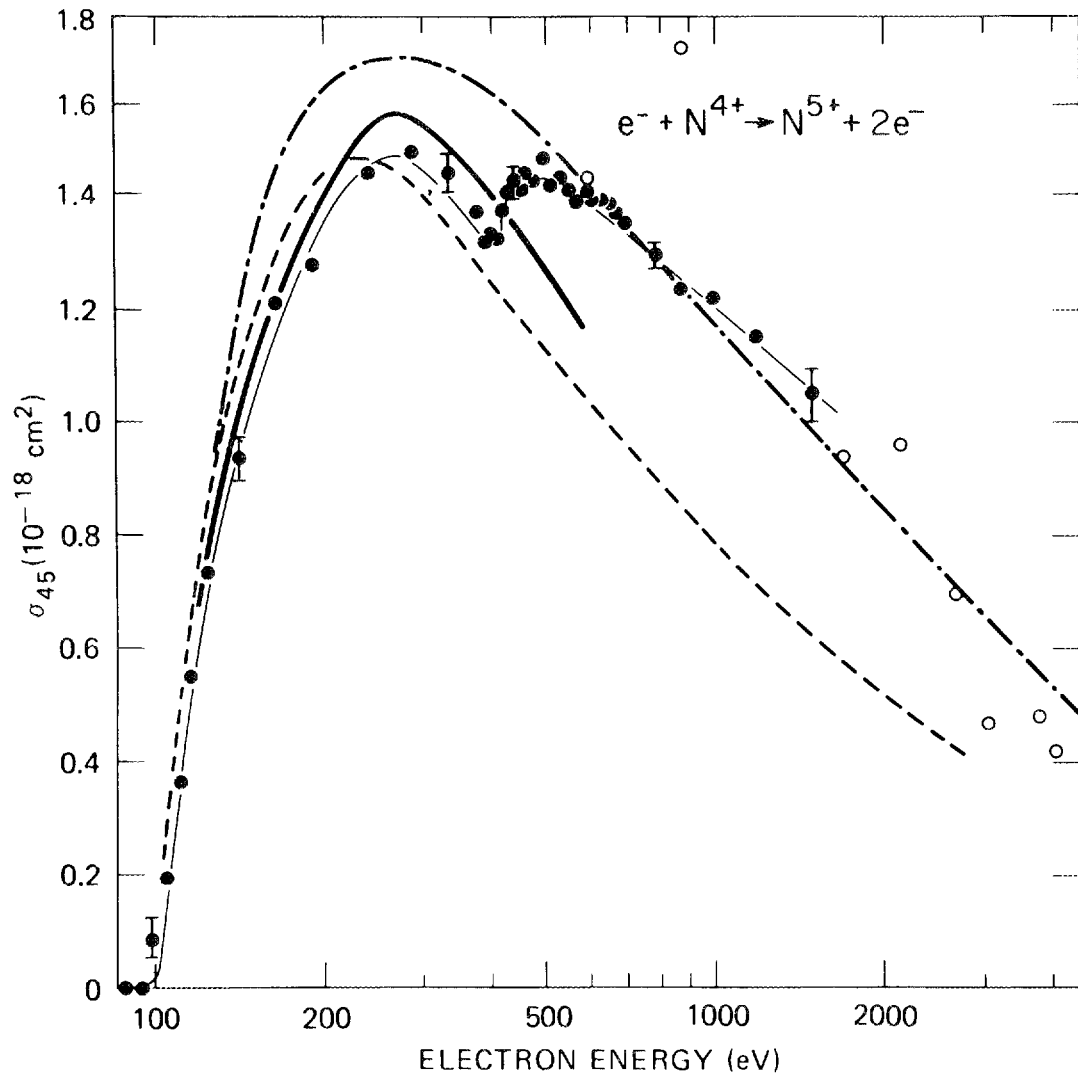


Fig. 3. Cross sections for electron impact ionization of N^{4+} . Connected solid points are present data with error bars at 90% confidence level statistics; open points are data of Donets and Ovsyannikov (Ref. 15); solid curve is Coulomb Born (Ref. 10); dashed curve is scaled Coulomb Born (Ref. 12); dot-dashed curve is Lotz (Ref. 6).

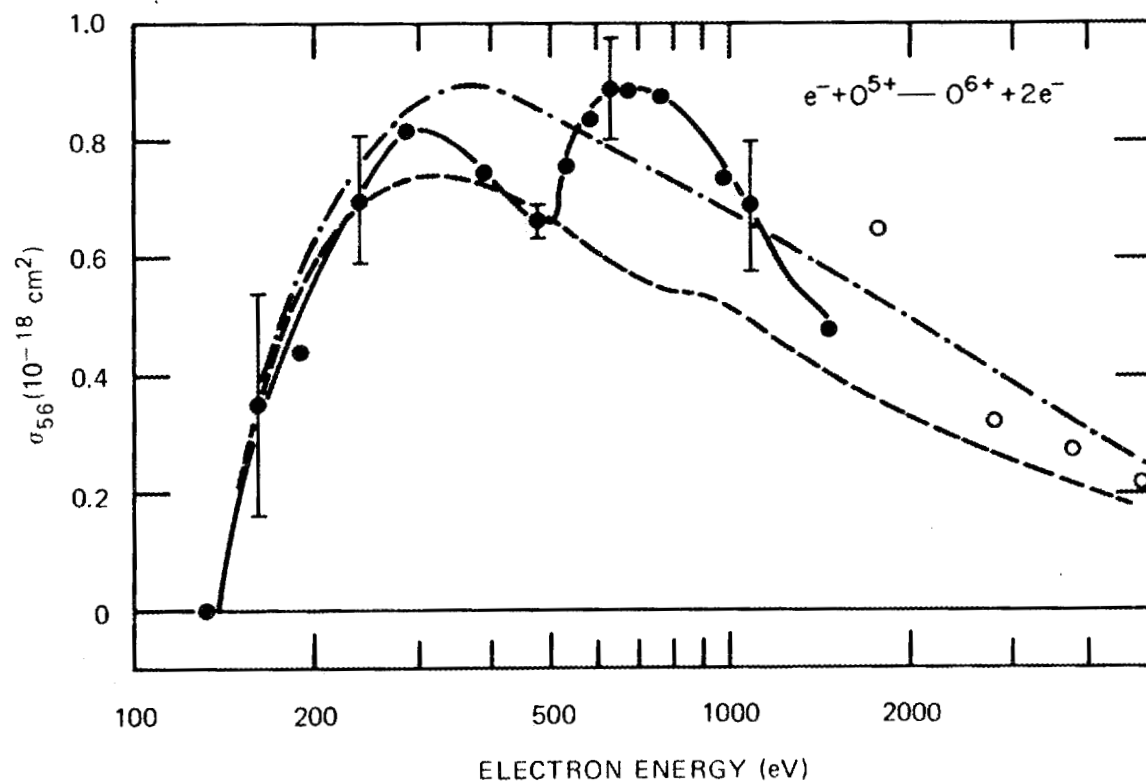


Fig. 4. Cross section for electron impact ionization of O^{5+} . Connected solid points are present data with error bars at 90% confidence level statistics; open points are data of Donets and Ovsyannikov (Ref. 15); dashed curve is scaled Coulomb Born (Ref. 12); dot-dashed curve is Lotz (Ref. 6).

ORNL-DWG 79-14124

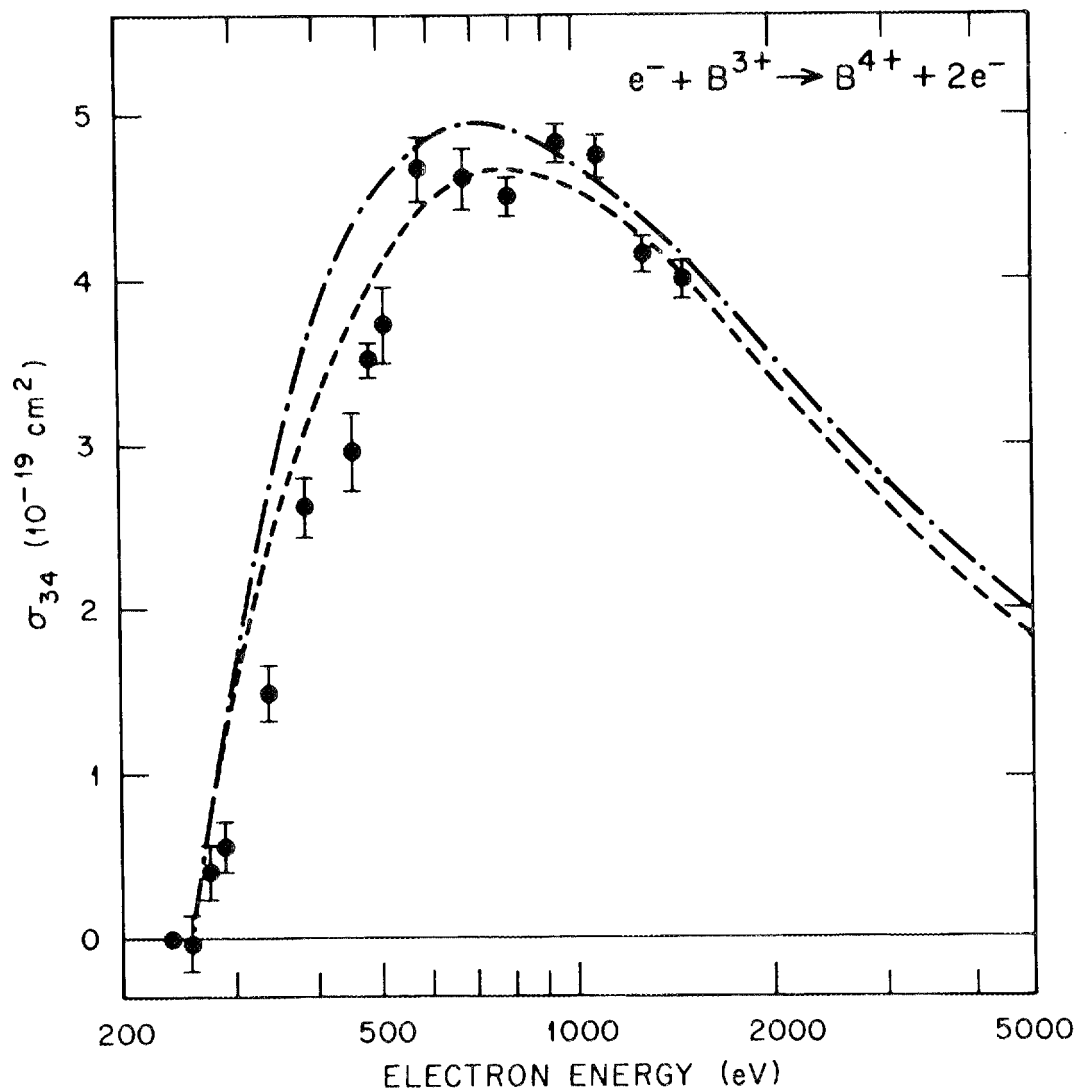


Fig. 5. Cross section for electron impact ionization of B^{3+} . Solid points are present data with error bars of one standard deviation on counting statistics; dashed curve is scaled Coulomb Born (Ref. 12); dot-dashed curve is Lotz (Ref. 6).

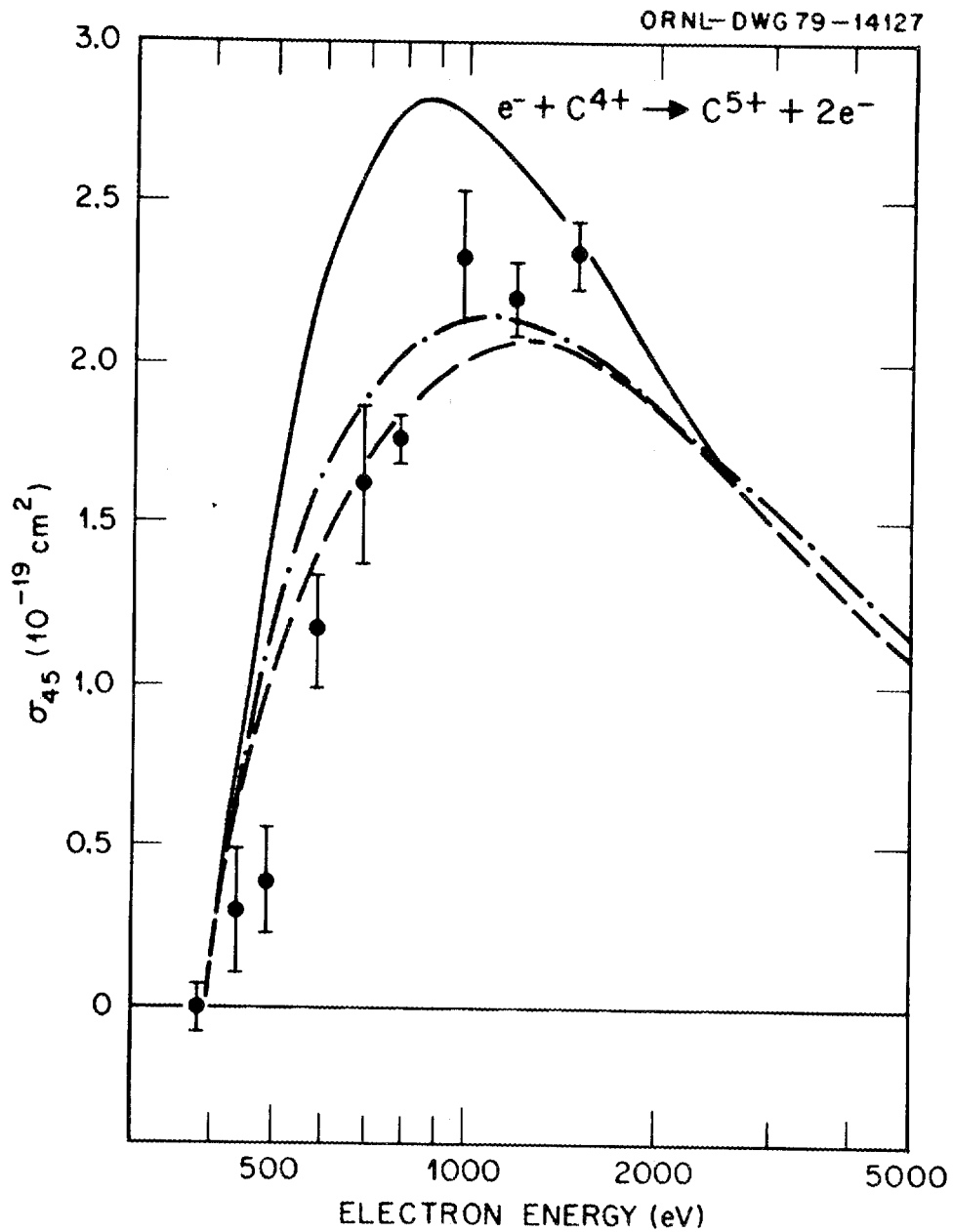


Fig. 6. Cross section for electron impact ionization of C^{4+} . Solid points are present data (error bars are one standard deviation statistics); dashed curve is scaled Coulomb Born (Ref. 12); dot-dashed curve is Lotz (Ref. 6); solid curve is classical theory calculated by Salop (Ref. 16).

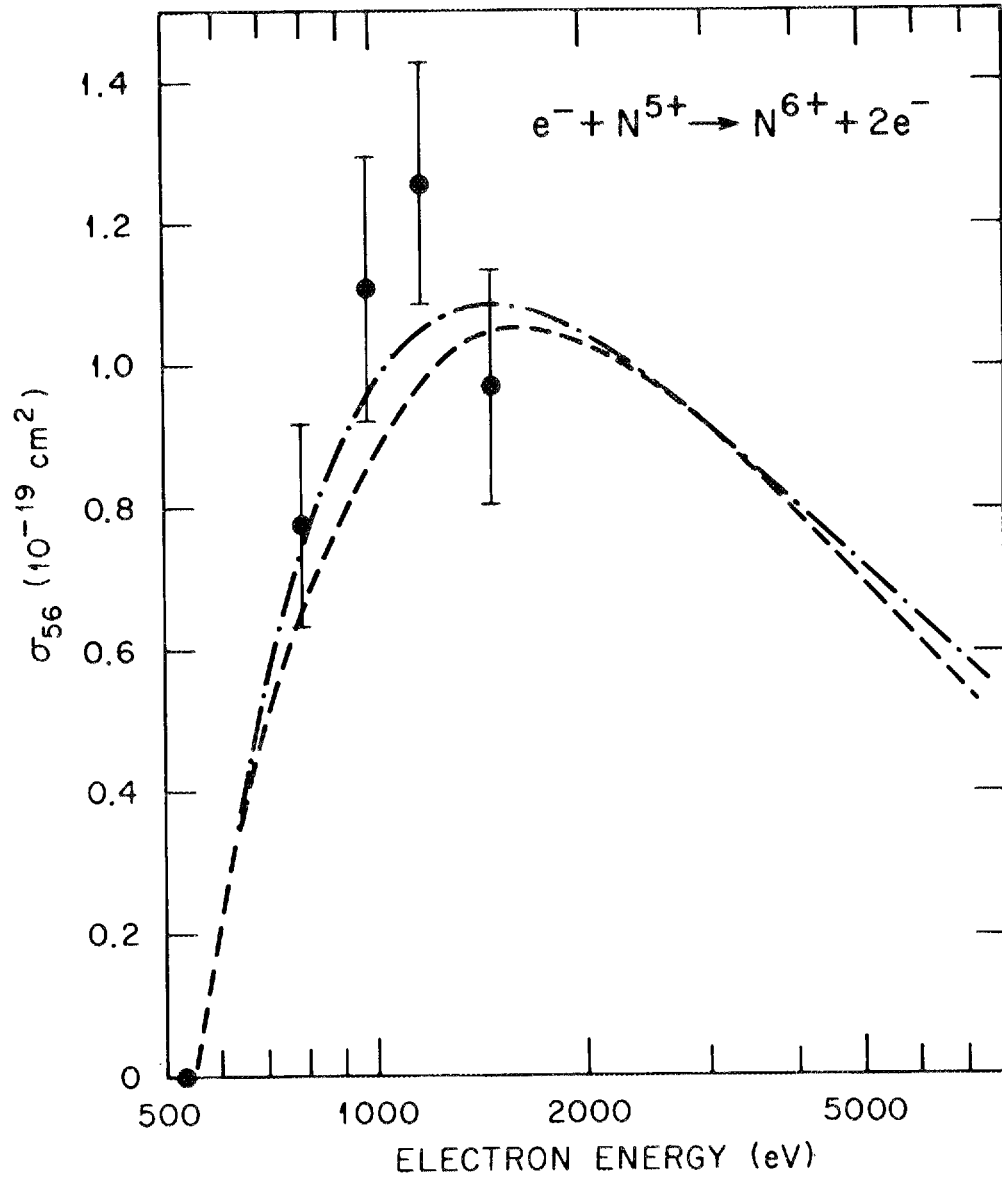


Fig. 7. Cross section for electron impact ionization of N^{5+} . Solid points are present data (error bars are one standard deviation statistics); dashed curve is scaled Coulomb Born (Ref. 2); dot-dashed curve is Lotz (Ref. 6).

ORNL-DWG 79-14125

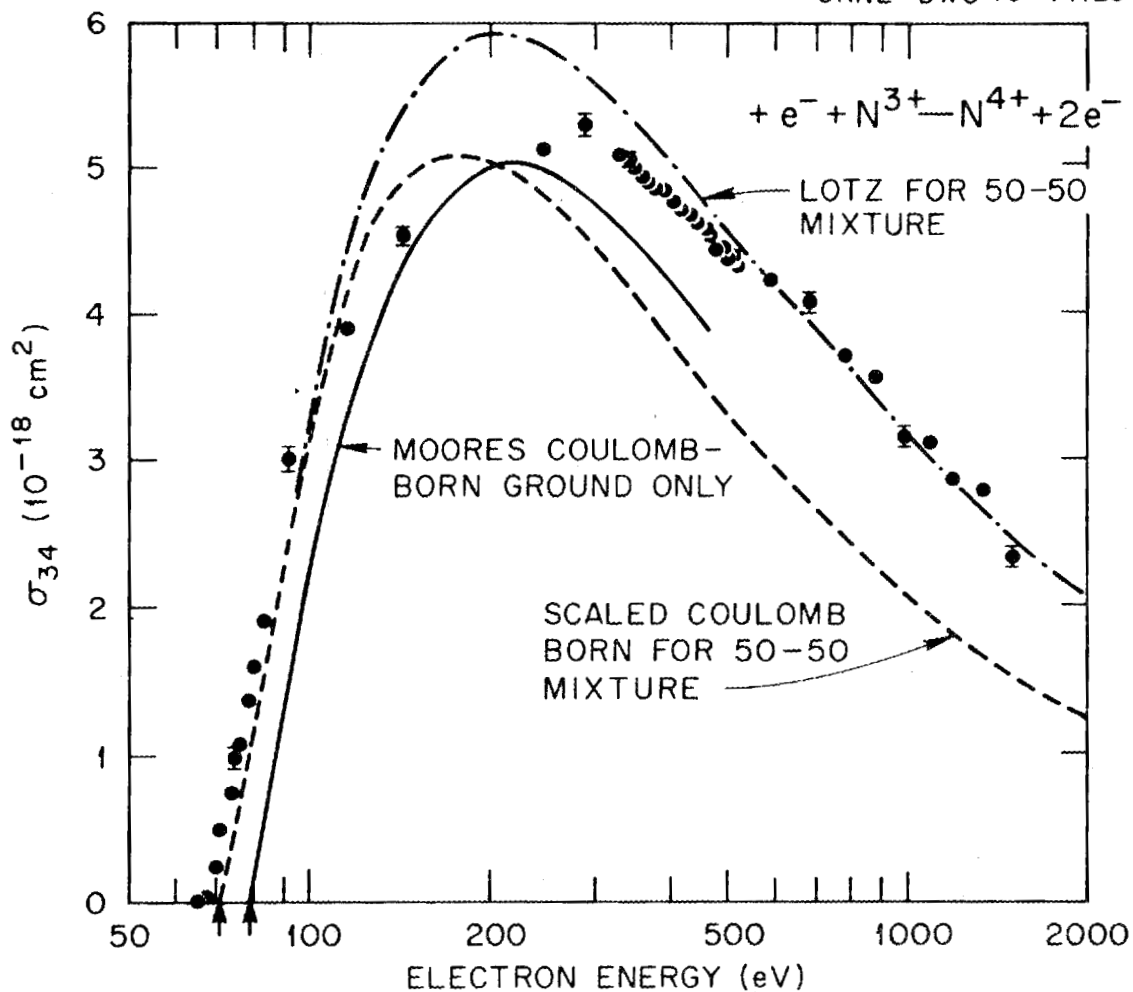


Fig. 8. Cross section for electron impact ionization of N^{3+} . Solid points are present data with estimated incident ion beam mixture of 50% $(1s^2 2s^2) \ ^1S$ ground state with threshold at 77.5 eV and 50% $(1s^2 2s 2p) \ ^3P$ metastable state with threshold at 69.1 eV (error bars are 90% confidence level statistics); solid curve is Coulomb Born by Moores (Ref. 10) for ground state ions; dashed curve is scaled Coulomb Born (Ref. 12) for 50-50 mixture of initial states; dot-dashed curve is Lotz (Ref. 6) for 50-50 mixture.

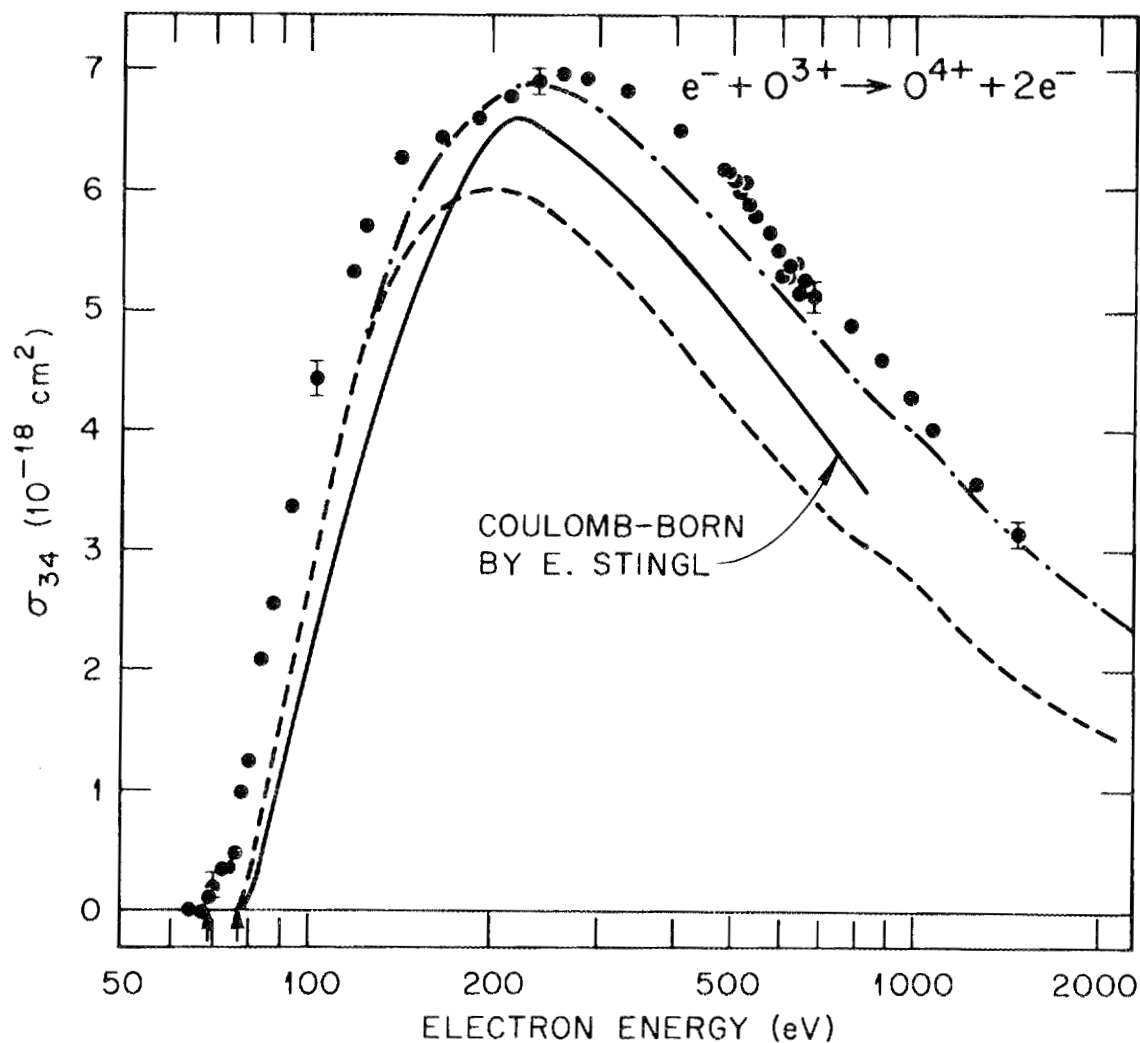


Fig. 9. Cross section for electron impact ionization of O^{3+} . Solid points are present data with estimated incident ion beam of 84% $(1s^2 2s^2 2p)^2 P$ ground state with threshold at 77.4 eV and 16% $(1s^2 2s 2p^2)^4 P$ metastable state with threshold at 68.6 eV (error bars are 90% confidence level statistics); solid curve is Coulomb Born with exchange by E. Stingl (Ref. 11) for ground state; dashed curve is scaled Coulomb Born (Ref. 12) for ground state; dot-dashed curve is Lotz (Ref. 6) for ground state.

ORNL-DWG 79-12011R2

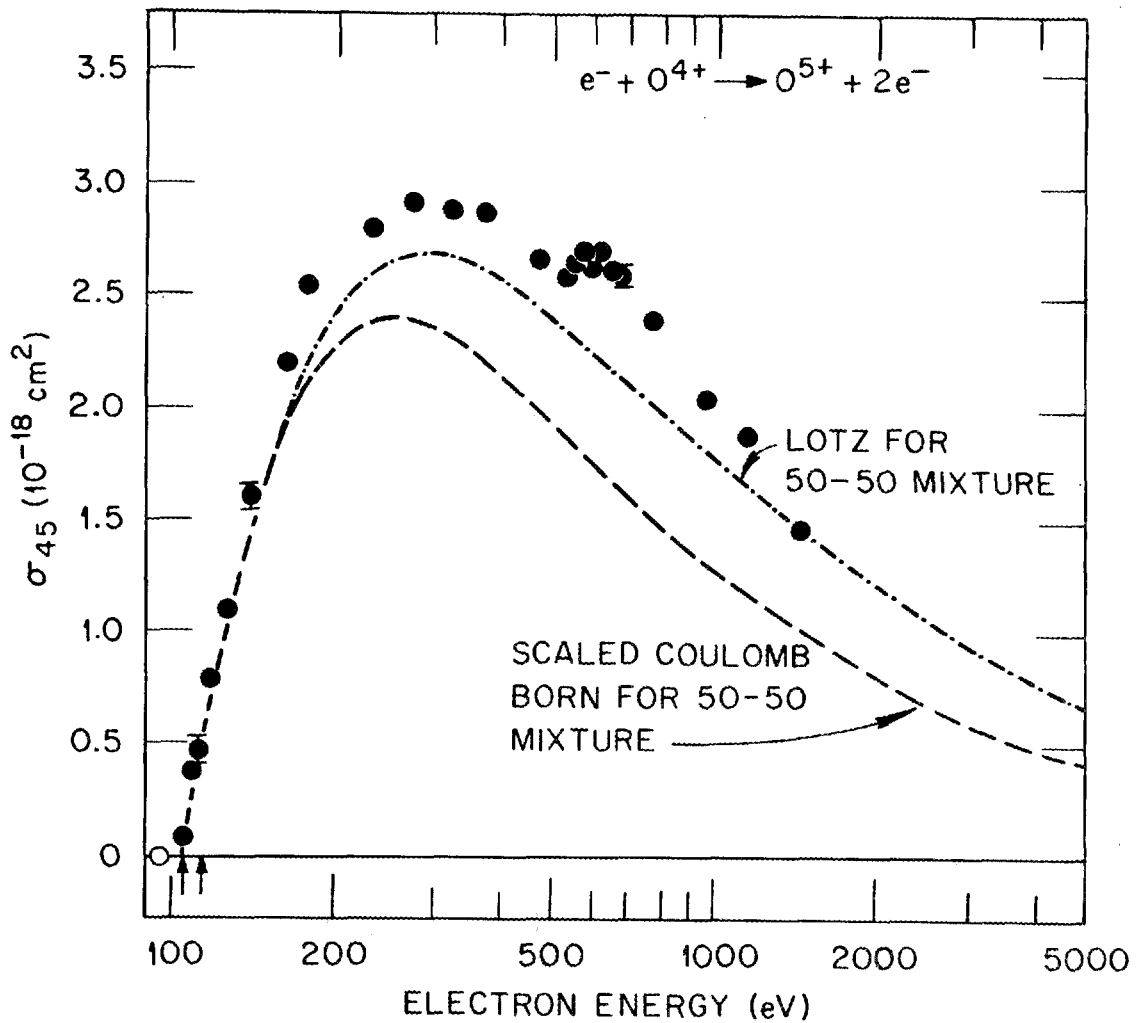


Fig. 10. Cross section for electron impact ionization of O^{4+} . Solid points are present data with estimated incident ion beam of 50% $(1s^2 2s^2) 1s$ ground state with threshold at 113.9 eV and 50% $(1s^2 2s 2p) 3p$ metastable state with threshold at 103.7 eV (error bars are 90% confidence level statistics); dashed curve is scaled Coulomb Born (Ref. 12) for 50-50 mixture; dot-dashed curve is Lotz (Ref. 6) for 50-50 mixture.

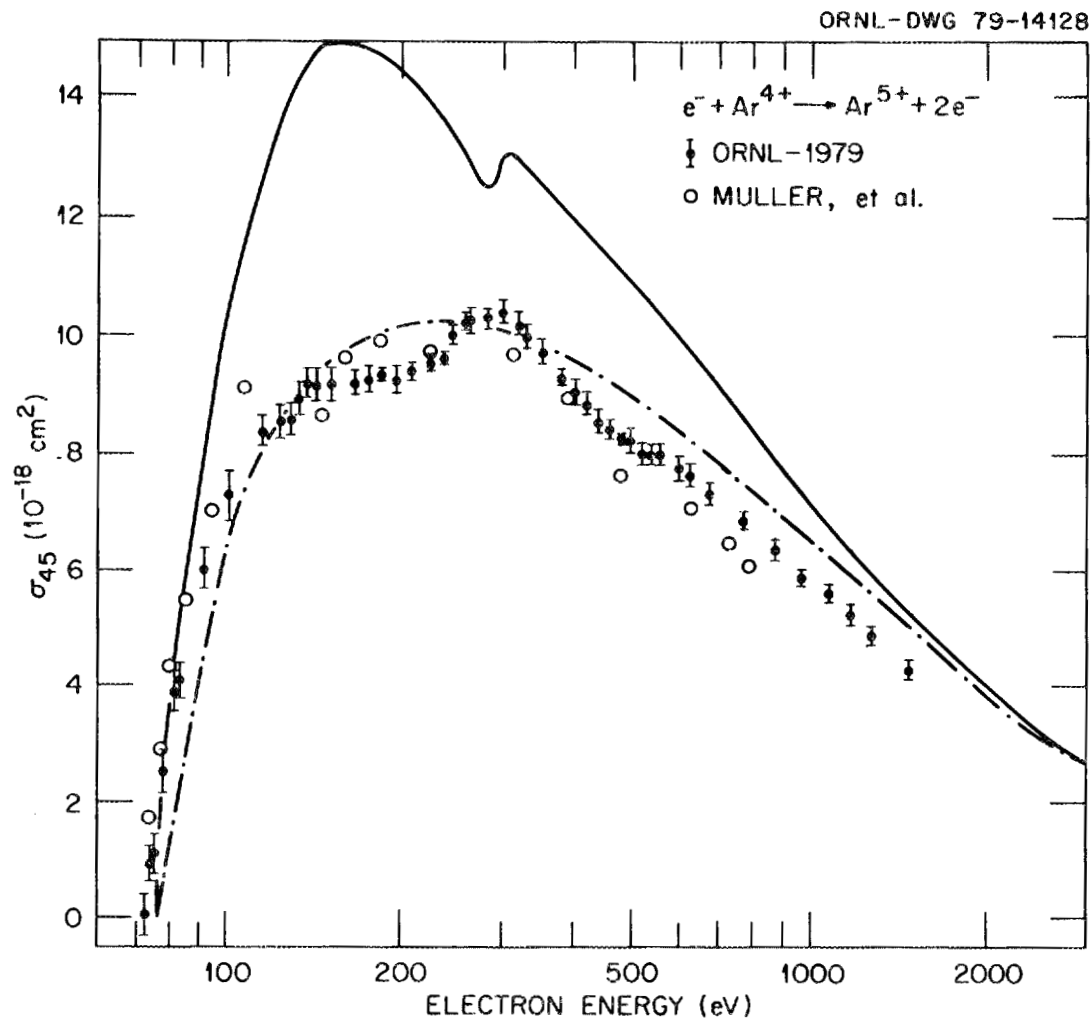


Fig. 11. Cross section for electron impact ionization of Ar^{4+} . Solid points are present data (error bars are 90% confidence level statistics); open points are data of Muller et al. (Ref. 17); dot-dashed curve is Lotz (Ref. 6); solid curve is classical theory calculated by Salop (Ref. 16).

2.2. Ionization Rates

Ionization rates for these ions in a plasma with Maxwellian electron temperature distribution have been calculated from the measured cross sections employing a computer code developed at JILA.²³ For convenience and most direct comparisons, the ionization rates for scaled-Coulomb-Born and Lotz theoretical estimates were also computed with the JILA rate code with discrete cross sections calculated according to the cross section formulas. As a check, the Lotz ionization rates obtained from the code have been compared for a few cases with the analytic expression:

$$\alpha = 3.0 \times 10^{-6} \sum_j \frac{r_j}{I_j \sqrt{KT}} E_1\left(\frac{I_j}{KT}\right) \text{ cm}^3/\text{sec}$$

where r_j is the number of electrons in subshell j , I_j is the ionization energy for electrons in subshell j (in eV), KT is the electron temperature in eV, E_1 is the exponential integral of index one, and α is the rate coefficient in cm^3/sec . The analytic formula agrees with the quoted Lotz ionization rates to between 1 and 5% for the cases checked. An analytic expression for the rates predicted by scaled Coulomb-Born is given in Ref. 12. The ionization rates are given in Fig. 12 for N^{4+} and in Tables 4-7 for all of the present cases.

The rates given in Tables 4-7 are for ionization out of the ground state except as noted for the Be-like ions. Thus the results are appli-

cable to plasmas of low density ($n_e \lesssim 10^{14} \text{ cm}^{-3}$) where excited states of these ions should not be abundant. The measured ionization rates of Kunze,²⁴ Kallne and Jones,²⁵ and Rowan and Roberts²⁶ which are shown on Fig. 12 were observed at densities near $n_e = 10^{16} \text{ cm}^{-3}$ where the presence of excited ion species in the plasma is significant. In Refs. 24-26 the measured rates are given and compared with the Lotz formula as corrected for excited states due to high plasma density. For the present comparison (Fig. 12) these measured rates have been reduced to represent ionization out of the ground state only. The reduction is the same percentage as given in Refs. 24-26 as an increase to the Lotz result in each specific case. Similar comparisons of present rates to plasma measured rates can be made for O^{5+} , C^{3+} , B^{3+} , and C^{4+} by adjustments of values given in Refs. 24-27.

Table 4. Ionization rates for Li-like ions in units of $10^{-9} \text{ cm}^3/\text{sec}$.

Temperature		C ³⁺ Rate			N ⁴⁺ Rate			O ⁵⁺ Rate		
10 ⁶ K	eV	Present	Scaled C-B	Lotz	Present	Scaled C-B	Lotz	Present	Scaled C-B	Lotz
0.2	17.2	0.042	0.052	0.058	0.003	0.004	0.004			
0.4	34.5	0.292	0.399	0.465	0.070	0.076	0.084	0.013	0.013	0.014
0.6	51.7	0.612	0.792	0.955	0.202	0.215	0.243	0.056	0.056	0.060
1.0	86.2	1.137	1.365	1.720	0.487	0.497	0.582	0.187	0.181	0.202
2.0	172	1.865	2.000	2.700	1.003	0.920	1.147	0.491	0.437	0.516
4.0	345	2.436	2.328	3.361	1.522	1.216	1.626	0.827	0.671	0.842
6.0	517	2.773	2.385	3.567	1.761	1.306	1.819	0.967	0.756	0.991
10	862	3.036	2.356	3.649	2.007	1.345	1.956	1.050	0.835	1.116
20	1720	2.888	2.172	3.507	2.008	1.296	1.967	1.026	0.862	1.166
50	4310	2.641	1.818	3.036	1.786	1.097	1.773	0.860	0.819	1.073
100	8620	2.327	1.527	2.599	1.530	0.931	1.548	0.727	0.733	0.940
600	51700	1.450	0.881	1.546	0.897	0.545	0.947	0.412	0.478	0.577

Table 5. Ionization rates for He-like ions in units of $10^{-10} \text{ cm}^3/\text{sec}$.

Temperature		B ³⁺ Rate			C ⁴⁺ Rate			N ⁵⁺ Rate		
10 ⁶ K	eV	Present	Scaled C-B	Lotz	Present	Scaled C-B	Lotz	Present	Scaled C-B	Lotz
0.2	17.2									
0.4	34.5	0.001	0.002	0.002						
0.6	51.7	0.022	0.033	0.036	0.001	0.001	0.001			
1.0	86.2	0.221	0.290	0.322	0.020	0.029	0.032	0.002	0.002	0.003
2.0	172	1.415	1.600	1.755	0.303	0.358	0.393	0.083	0.077	0.084
4.0	345	3.813	3.963	4.235	1.322	1.348	1.448	0.587	0.469	0.506
6.0	517	5.329	5.390	5.694	2.194	2.141	2.264	1.057	0.886	0.940
10	862	6.887	6.791	7.144	3.260	3.101	3.235	1.676	1.492	1.557
20	1720	8.049	7.704	8.176	4.208	3.968	4.139	2.329	2.173	2.253
50	4310	8.060	7.384	8.116	4.441	4.251	4.463	2.694	2.527	2.663
100	8620	7.379	6.579	7.352	4.119	3.929	4.224	2.645	2.445	2.626
600	51700	4.834	4.100	4.822	2.718	2.620	2.914	1.924	1.720	1.908

Table 6. Ionization rates for Be-like ions with 50-50 mixture of ground state and metastable state ions in units of 10^{-9} cm³/sec.

Temperature		N ³⁺ Rate			O ⁴⁺ Rate		
10 ⁶ K	eV	Present	Scaled C-B	Lotz	Present	Scaled C-B	Lotz
0.2	17.2	0.059	0.048	0.049	0.004	0.003	0.003
0.4	34.5	0.524	0.487	0.528	0.110	0.091	0.090
0.6	51.7	1.127	1.077	1.203	0.346	0.289	0.298
1.0	86.2	2.179	2.029	2.365	0.897	0.742	0.801
2.0	172	3.738	3.143	3.951	1.907	1.481	1.740
4.0	345	4.807	3.671	5.014	2.783	2.001	2.572
6.0	517	5.275	3.726	5.325	3.104	2.147	2.887
10	862	5.323	3.593	5.424	3.260	2.168	3.077
20	1720	5.101	3.221	5.182	3.123	2.043	3.074
50	4310	4.400	2.559	4.442	2.737	1.702	2.741
100	8620	3.758	2.083	3.784	2.331	1.424	2.386
600	51700	2.228	1.131	2.232	1.371	0.812	1.459

Table 7. Ionization rates for O^{3+} and Ar^{4+} in units of $10^{-9} \text{ cm}^3/\text{sec}$

Temperature		O^{3+} Rate			Ar^{4+} Rate	
10^6 K	eV	Present	Scaled C-B	Lotz	Present	Lotz
0.2	17.2	0.059	0.035	0.034	0.101	0.063
0.4	34.5	0.616	0.466	0.476	0.982	0.783
0.6	51.7	1.406	1.125	1.196	2.150	1.885
1.0	86.2	2.808	2.285	2.559	4.160	3.914
2.0	172	4.894	3.787	4.575	7.031	7.012
4.0	345	6.348	4.587	6.023	9.071	9.535
6.0	517	6.906	4.687	6.482	9.630	10.49
10	862	6.941	4.507	6.686	9.604	11.08
20	1720	6.476	3.919	6.443	9.125	10.97
50	4310	5.371	2.927	5.520	7.641	9.678
100	8620	4.465	2.319	4.778	6.395	8.364
600	51700	2.514	1.142	2.838	3.651	5.042

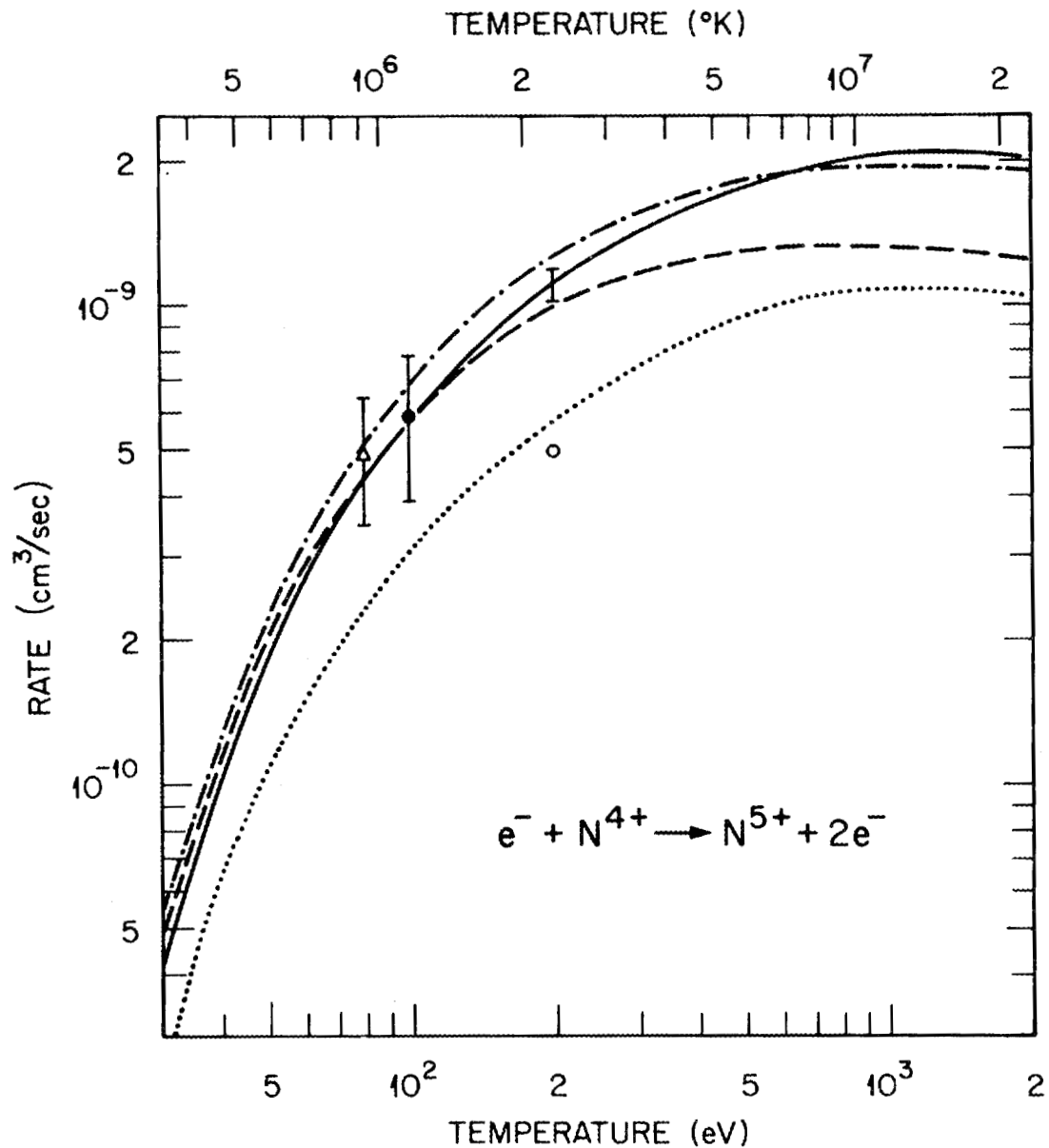


Fig. 12. Ionization rates for ground state N^{4+} as a function of plasma electron temperature. Solid curve is present result; open circle is plasma observed rate of Kunze (Ref. 24); solid circle is plasma observed rate of Kallne and Jones (Ref. 25); open triangle is plasma observed rate of Rowan and Roberts (Ref. 26); long-dashed curve is scaled Coulomb Born (Ref. 12); dot-dashed curve is Lotz (Ref. 6); and dotted curve is ECIP calculation of Summers (Ref. 9). Error bar on present result at 200 eV is cross section uncertainty at high confidence (equivalent to 90% confidence level).

3. Conclusion

Except for the C^{3+} case, the simple Lotz formula is remarkably accurate. However, this conclusion may not apply to untested cases and may be accidental for the present data. For N^{4+} and O^{5+} cases the scaled-Coulomb-Born calculations are better than the Lotz formula at low energies, and only the occurrence of the excitation-autoionization contribution (not included in any of the theories) brings about better agreement of experiment and Lotz formula at higher energies. For Be-like O^{4+} and N^{3+} the Lotz formula appears best, but this may again be accidental and applicable only to Be-like ions. For the He-like cases (by far the most difficult experiments) the difference between theories cannot be tested by the data. Nevertheless, the Lotz formula is found to be more accurate than the factor of two uncertainty frequently ascribed to it. While detailed Coulomb-Born calculations including such effects as excitation-autoionization may eventually prove to be the most accurate theory, the approximate scaled-Coulomb-Born results are not better than the simple Lotz formula for the present cases.

References

1. M. L. Mallory and D. H. Crandall, IEEE Trans. Nucl. Sci. NS23, 1069 (1976).
2. P. O. Taylor, K. T. Dolder, W. E. Kauppila, and G. H. Dunn, Rev. Sci. Instrum. 45, 588 (1975).
3. D. H. Crandall, R. A. Phaneuf, and P. O. Taylor, Phys. Rev. A 18, 1911 (1978).
4. D. H. Crandall, R. A. Phaneuf, B. E. Hasselquist, and D. C. Gregory, J. Phys. B 12, L249 (1979).
5. J. J. Thomson, Philos. Mag. 23, 449 (1912).
6. W. Lotz, Z. Phys. 216, 241 (1968).
7. A. Burgess, H. P. Summers, D. M. Cochrane, R. W. P. McWhirter, Mon. Not. R. Astron. Soc. 179, 275 (1977).
8. W. D. Barfield, IEEE Trans. Plasma Sci. PS-6, 71 (1978).
9. H. P. Summers, Mon. Not. R. Astron. Soc. 169, 663 (1974).
10. D. L. Moores, J. Phys. B 11, 403 (1978).
11. E. Stigl, J. Phys. B 5, 1160 (1972).
12. L. B. Golden and D. H. Sampson, J. Phys. B 10, 2229 (1977).
13. E. Clementi and C. Roetti, At. Nucl. Data Tables 14, 177 (1974).
14. N. H. Magee, Jr., J. B. Mann, A. L. Merts, and W. D. Robb, Los Alamos Scientific Laboratory Report LA6691 M.S. (1977), pp. 109-112.
15. E. D. Donets and V. P. Ovsyannikov, Joint Institute of Nuclear Research, Dubna, Report No. P7-10780 (1977) (translation ORNL-tr-4616 available from Technical Information Center, P. O. Box 62, Oak Ridge, TN 37830).

16. A. Salop, Phys. Rev. A 14, 2095 (1976).
17. A. Muller, E. Salzborn, R. Frodl, R. Becker, H. Klein, and H. Winter, "Absolute Experimental Cross Sections for the Electron Impact Ionization of Argon Ions," submitted to J. Phys. B.
18. D. H. Crandall and R. A. Phaneuf, Abstracts of Contributed Papers of XI ICPEAC, Kyoto, Japan, to be published (1979).
19. O. Bely, J. Phys. B 1, 23 (1968).
20. Y. Hahn, Phys. Rev. A 18, 1029 (1978).
21. R. J. W. Henry, J. Phys. B 12, L309 (1979).
22. R. D. Cowan and J. B. Mann, "Contribution of Autoionization to Total Ionization Rates," Astrophys. J., accepted (1979).
23. D. H. Crandall, G. H. Dunn, A. Gallagher, D. G. Hummer, C. V. Kunasz, D. Leep, and P. O. Taylor, Astrophys. J. 191, 789 (1974).
24. H.-J. Kunze, Phys. Rev. A 3, 937 (1971).
25. E. Kallne and L. A. Jones, J. Phys. B 10, 3637 (1977).
26. W. L. Rowan and J. R. Roberts, Phys. Rev. A 19, 90 (1979).
27. R. U. Datla, L. J. Nugent, and H. R. Griem, Phys. Rev. A 14, 979 (1976).

INTERNAL DISTRIBUTION

ORNL/TM-7020

- | | |
|------------------------|-------------------------------------|
| 1. C. F. Barnett | 27. F. W. Meyer |
| 2. C. Bottcher | 28. C. D. Moak |
| 3. J. D. Callen | 29. D. J. Pegg |
| 4. L. G. Christophorou | 30. R. A. Phaneuf |
| 5-14. D. H. Crandall | 31. J. A. Rome |
| 15. E. C. Crume | 32. I. A. Sellin |
| 16. P. F. Dittner | 33. P. H. Stelson |
| 17. W. Dress | 34. J. Sheffield |
| 18. W. R. Garrett | 35. R. S. Thoe |
| 19. G. R. Haste | 36. J. W. Wooten |
| 20. S. W. Hawthorne | 37-38. Central Research Library |
| 21. J. T. Hogan | 39. Fusion Energy Library |
| 22. R. C. Isler | 40-41. Laboratory Records |
| 23. E. F. Jaeger | 42. Laboratory Records, ORNL-RC |
| 24. M. O. Krause | 43. ORNL Document Reference Section |
| 25. J. A. Martin | 44. ORNL Patent Office |
| 26. G. S. McNeilly | 45. ORNL Y-12 Technical Library |

EXTERNAL DISTRIBUTION

46. W. D. Barfield, Los Alamos Scientific Laboratory, Los Alamos, NM 87545
47. E. C. Beaty, JILA, University of Colorado, Boulder, CO 80309
48. R. Bengtson, University of Texas, Austin, TX 78712
49. K. H. Burrell, General Atomic Company, San Diego, CA 92138
50. J. Callaway, Louisiana State University, Baton Rouge, LA 70803
51. A. Chutjian, Jet Propulsion Laboratory, California Institute of Technology, Pasadena, CA 91103
52. Y. P. Chong, University of Maryland, College Park, MD 20742
53. R. D. Cowan, Los Alamos Scientific Laboratory, Los Alamos, NM 87544
54. A. Dalgarno, Harvard College Observatory, Cambridge, MA 02138
55. K. T. Dolder, University of Newcastle upon Tyne, Newcastle-on-Tyne, England
56. E. D. Donets, Joint Institute of Nuclear Research, Dubna, U.S.S.R.
57. P. Drake, Lawrence Livermore Laboratory, Livermore, CA 94550
58. G. H. Dunn, JILA, University of Colorado, Boulder, CO 80309
59. H. B. Gilbody, The Queen's University of Belfast, Belfast, Northern Ireland
60. G. H. Gillespie, Physical Dynamics, Inc., La Jolla, CA 92038
61. L. B. Golden, The Pennsylvania State University, Dunmore, PA 18512
62. D. C. Gregory, Brookhaven National Laboratory, Upton, NY 11973
63. H. R. Griem, University of Maryland, College Park, MD 20742
64. Y. Hahn, University of Connecticut, Storrs, CT 06457
65. M. F. A. Harrison, Culham Laboratory, Abingdon, Oxfordshire, England
66. R. J. W. Henry, Louisiana State University, Baton Rouge, LA 70803
67. E. Hinnoy, Princeton Plasma Physics Laboratory, Princeton, NJ 08540
68. J. Hiskes, Lawrence Livermore Laboratory, Livermore, CA 94550

69. Y. Itikawa, Institute of Space and Aeronautical Science, University of Tokyo, Tokyo, Japan
70. K. W. Jones, Brookhaven National Laboratory, Upton, NY 11973
71. L. A. Jones, Los Alamos Scientific Laboratory, Los Alamos, NM 87545
72. E. Källne, University of Virginia, Charlottesville, VA 22501
73. Y.-K. Kim, Argonne National Laboratory, Argonne, IL 60439
74. H. Klein, Institut für Angewandte Physik, Universität Frankfurt, Frankfurt, West Germany
75. J. L. Kohl, Center for Astrophysics, Cambridge, MA 92138
76. H. J. Kunze, Institut für Exp.-Physics, Ruhr-Universität, Bochum, West Germany
77. J. H. Macek, University of Nebraska, Lincoln, NE 68588
78. J. B. Mann, Los Alamos Scientific Laboratory, Los Alamos, NM 87545
79. J. V. Martinez, U. S. Department of Energy, Washington, DC 20545
80. R. McCarroll, Université de Bordeaux I, Talence, France
81. R. McCray, JILA, University of Colorado, Boulder, CO 80309
82. W. McGowan, University of Western Ontario, London, Canada
83. R. W. P. McWhirter, Culham Laboratory, Abingdon, Oxfordshire, England
84. M. Menendez, University of Georgia, Atlanta, GA 30602
85. A. L. Merts, Los Alamos Scientific Laboratory, Los Alamos, NM 87544
86. D. Moores, University College, London, England
87. W. Moos, Johns Hopkins University, Baltimore, MD 21218
88. P. Moriette, Association Euratom - CEA sur la Fusion, Paris, France
89. D. W. Norcross, JILA, University of Colorado, Boulder, CO 80309
90. J. T. Park, University of Missouri-Rolla, Rolla, MO 65401
91. J. Peek, Sandia Laboratories, Albuquerque, NM 87115
92. M. S. Pindzola, Auburn University, Auburn, AL 36830
93. D. E. Post, Princeton Plasma Physics Laboratory, Princeton, NJ 08450
94. D. H. Priester, U. S. Department of Energy, Washington, DC 20545
95. R. V. Pyle, Lawrence Berkeley Laboratory, Berkeley, CA 94720
96. W. D. Robb, Los Alamos Scientific Laboratory, Los Alamos, NM 87545
97. J. R. Roberts, National Bureau of Standards, Washington, DC 20234
98. T. Romesser, TRW Inc., Redondo Beach, CA 90278
99. L. Roszman, National Bureau of Standards, Washington, DC 20234
100. W. L. Rowan, National Bureau of Standards, Washington, DC 20234
101. E. Salzborn, Liebig-Universität, Giessen, West Germany
102. D. H. Sampson, The Pennsylvania State University, University Park, PA 16802
103. T. Sharp, Lockheed - Palo Alto Research Laboratory, Palo Alto, CA 94304
104. P. Stone, U. S. Department of Energy, Washington, DC 20545
105. B. Tartar, Lawrence Livermore Laboratory, Livermore, CA 94550
106. P. O. Taylor, Center for Astrophysics, Cambridge, MA 02138
107. D. Thomson, Los Alamos Scientific Laboratory, Los Alamos, NM 87545
108. B. P. Tsai, University of Minnesota, Duluth, MN 55812
109. L. A. Vainstein, P. N. Lebedev Physical Institute, Moscow, U.S.S.R.
110. H. Winter, Institut für Allgemeine Physik, Technische Universität Wien, Wien, Austria
111. S. M. Younger, National Bureau of Standards, Washington, DC 20234
112. Asst. Manager, Energy Research and Development, DOE-ORO
- 113-139. Technical Information Center